19

Complex Representation

The shortest path between two truths in the real domain passes through the complex domain.

Jacques Hadamard (1865–1963)

The recognition that complex numbers admit a geometrical interpretation, as points in the Euclidean plane, was a critical step in securing their widespread acceptance (see §4.1). The "geometric algebra" of points in $\mathbb{R}^2$ defined by the arithmetic rules for complex numbers allows us to *multiply* and *divide* points, as well as adding or subtracting them in the usual vector sense. However, the systematic use of complex numbers as a means of exploring analytic geometry in $\mathbb{R}^2$ has received less attention than it deserves — *The Advanced Geometry of Plane Curves and Their Applications*[1] by C. Zwikker [480] seems to be the only treatise that consistently employs this approach.

The complex representation of $\mathbb{R}^2$ is especially valuable in the analysis of planar PH curves, since it offers a simple and elegant characterization of the Pythagorean hodograph property. Any task performed in terms of the complex representation could, in principle, be accomplished using only real variables. However, on account of the useful geometrical insights it provides — and also significant savings in the cost of formulating and solving the systems of non–linear equations associated with interpolation problems (Chaps. 25 and 27) — we shall rely extensively on the complex representation of planar PH curves henceforth. An analogous representation for spatial PH curves (in terms of the *quaternions* rather than complex numbers) is developed in Chap. 22.

In this chapter, we use the complex formulation to establish a one–to–one correspondence between regular PH curves and "ordinary" polynomial curves in $\mathbb{R}^2$, to characterize the control polygons of planar PH curves, and to verify their rotation invariance and study their intrinsic shape properties.

---

[1] Regrettably, this book has not survived even as a *Dover* reprint. Another useful source, though not directly concerned with the complex representation of plane curves, is Schwerdtfeger's *Geometry of Complex Numbers* [397].

19.1 Complex Curves and Hodographs

Associating the point (x, y) of the Euclidean plane with the complex number $x + \mathrm{i}\, y$, we regard these two quantities as interchangeable and use a single bold character $\mathbf{z}$ to denote both. Expressions such as $\mathbf{z}_1 \pm \mathbf{z}_2$, $\mathbf{z}_1\mathbf{z}_2$, $\mathbf{z}_1/\mathbf{z}_2$ follow the usual rules of complex arithmetic (see §4.2), while $\mathbf{z}_1 \cdot \mathbf{z}_2$ and $\mathbf{z}_1 \times \mathbf{z}_2$ denote the scalar and vector products. Complex variables may also appear as arguments of transcendental functions — $\sin(\mathbf{z})$, $\cos(\mathbf{z})$, $\exp(\mathbf{z})$, $\log(\mathbf{z})$, etc.

A plane parametric curve can be specified by a complex–valued function $\mathbf{r}(t)$ defined on a given (possibly infinite) domain $t \in [\,a, b\,]$ of a real variable t. For example, $\mathbf{r}(t) = \mathbf{a}_1 t + \mathbf{a}_0$ and $\mathbf{r}(t) = \mathbf{a}_2 t^2 + \mathbf{a}_1 t + \mathbf{a}_0$ define a straight line and a parabola, respectively, while a circle with center $\mathbf{c}$ and radius r can be written as $\mathbf{r}(t) = \mathbf{c} + r\,\mathrm{e}^{\mathrm{i}t}$ for $0 \le t < 2\pi$. Perhaps less obvious is the fact that circles may also be described by the fractional linear (Möbius) form

$$\mathbf{r}(t) \;=\; \frac{\mathbf{a}\,t + \mathbf{b}}{\mathbf{c}\,t + \mathbf{d}}\,,$$

and that, for real α, the expressions

$$\mathbf{r}(t) \;=\; \cos(t + \mathrm{i}\,\alpha) \qquad \text{and} \qquad \mathbf{r}(t) \;=\; \cos(\alpha + \mathrm{i}\,t)$$

define an ellipse and a hyperbola, respectively. See [480] for a wealth of further details on complex representations of plane curves and their properties.

For our purposes, the most interesting aspect of such representations is the ability to create new curves from any given curve by “distorting” the complex plane in which it resides using a *conformal map* defined by an analytic function of $\mathbf{z}$ (see §4.5 for the definition and basic properties of such maps). Our concern here is more subtle than the *direct* deformation of planar curves by means of conformal maps. Instead, we introduce a mapping of the *hodograph plane* — the plane in which the derivative $\mathbf{r}'(t)$ of a parametric curve $\mathbf{r}(t)$ resides. By this scheme, we establish a one–to–one correspondence[2] between the sets of regular PH curves and of regular “ordinary” polynomial curves, which offers a framework for comparing and contrasting their properties.

Consider a polynomial curve in the complex plane specified in Bézier form

$$\mathbf{r}(t) \;=\; \sum_{k=0}^{n} \mathbf{p}_k \binom{n}{k} (1-t)^{n-k} t^k\,, \quad t \in [\,0, 1\,]\,, \tag{19.1}$$

where the complex values $\mathbf{p}_k = x_k + \mathrm{i}\, y_k$, $k = 0, \ldots, n$ define the control points. The usual control polygon features — convex–hull confinement, the variation–diminishing property, and the subdivision and degree–elevation algorithms — carry over directly to the complex representation. The hodograph $\mathbf{w}(t) = \mathbf{r}'(t)$ of the curve (19.1) can be expressed as a complex Bézier curve of degree $n - 1$,

[2] Note that $\mathbf{r}(t)$ is uniquely determined by $\mathbf{r}'(t)$, modulo a translation corresponding to the integration constant.

$$\mathbf{w}(t) \;=\; \sum_{k=0}^{n-1} \mathbf{w}_k \binom{n-1}{k} (1-t)^{n-1-k} t^k \,, \quad t \in [\,0,1\,] \,, \tag{19.2}$$

with control points given by

$$\mathbf{w}_k \;=\; n\Delta\mathbf{p}_k \;=\; n\,(\mathbf{p}_{k+1} - \mathbf{p}_k)\,, \quad k = 0,\ldots,n-1\,.$$

The forward differences $\Delta\mathbf{p}_k = \mathbf{p}_{k+1} - \mathbf{p}_k$ define the n directed "legs" of the control polygon. For clarity, we regard curves and their hodographs as residing in two separate complex planes, $\mathbf{z} = x + \mathrm{i}\,y$ and $\mathbf{w} = u + \mathrm{i}\,v$, respectively.

19.2 One–to–one Correspondence

Using $\mathbb{C}$ as a representation for $\mathbb{R}^2$, let Π be the set of all regular polynomial curves, and $\hat{\Pi}$ be the set of all regular PH curves. By a regular curve, we mean a *specific parameterization* of such a curve (see Remark 19.2). To assess how "flexible" PH curves are, it is useful to characterize the relationship between these two sets. Although Π and $\hat{\Pi}$ are both infinite sets — they include curves of *arbitrary* degree — it is clear that $\hat{\Pi} \subset \Pi$, since any regular PH curve is certainly a regular polynomial curve, but there are regular polynomial curves whose hodographs are *not* Pythagorean (e.g., the parabola $\mathbf{r}(t) = t + \mathrm{i}\,t^2$). We introduce a simple three–stage procedure P that transforms any differentiable plane curve $\mathbf{r}(t)$ into a new curve $\hat{\mathbf{r}}(t)$.

$$\boxed{\textbf{procedure } P \,:\; \mathbf{r}(t) \;\rightarrow\; \hat{\mathbf{r}}(t)}$$

1. differentiate the given curve $\mathbf{r}(t)$
   to obtain its hodograph $\mathbf{w}(t) = \mathbf{r}'(t)\,$;
2. apply the conformal map $\mathbf{w} \rightarrow \mathbf{w}^2$ to
   the hodograph plane, giving $\hat{\mathbf{w}}(t) = \mathbf{w}^2(t)\,$;
3. integrate the transformed hodograph $\hat{\mathbf{w}}(t)$
   to obtain the new curve $\hat{\mathbf{r}}(t) = \int \hat{\mathbf{w}}(t)\,\mathrm{d}t\,$.

In this procedure, translational freedoms are fixed by taking $\mathbf{r}(0) = \hat{\mathbf{r}}(0) = 0$.

Proposition 19.1 *P defines a bijective map, or one–to–one correspondence, between the sets Π and $\hat{\Pi}$ of regular polynomial curves and regular PH curves.*

Proof : Let $\mathbf{r}(t) = x(t) + \mathrm{i}\,y(t)$ be a regular polynomial curve with hodograph $\mathbf{w}(t) = u(t) + \mathrm{i}\,v(t)$, where $u = x'$ and $v = y'$. Since $\mathbf{w}(t)$ does not pass through the origin, we must have $\gcd(u,v) =$ constant. Step 2 gives

$$\hat{\mathbf{w}}(t) \;=\; \mathbf{w}^2(t) \;=\; u^2(t) - v^2(t) \;+\; \mathrm{i}\,2\,u(t)v(t)$$

for the transformed hodograph, which is of Pythagorean form with u and v relatively prime. Integrating $\hat{\mathbf{w}}(t)$ then gives, modulo a translation, a unique regular PH curve $\hat{\mathbf{r}}(t)$ corresponding to $\mathbf{r}(t)$. Conversely, let $\hat{\mathbf{r}}(t)$ be a regular PH curve. Its hodograph must be of the form $\hat{\mathbf{w}}(t) = u^2(t) - v^2(t) + \mathrm{i}\, 2\, u(t)v(t)$, where $\gcd(u, v) = $ constant. The inverse to step 2 transforms $\hat{\mathbf{w}}(t)$ into

$$\mathbf{w}(t) \;=\; \sqrt{\hat{\mathbf{w}}(t)} \;=\; \pm\, [\, u(t) + \mathrm{i}\, v(t)\,]\,, \tag{19.3}$$

a hodograph that does not traverse the origin. Integrating $\mathbf{w}(t)$ gives, modulo translation, a unique regular polynomial curve $\mathbf{r}(t)$ corresponding to $\hat{\mathbf{r}}(t)$ — the *sense* of the parametric flow along $\mathbf{r}(t)$ is arbitrary, corresponding to the sign ambiguity on taking the complex square root. ∎

Note that, in general, the inverse map $\mathbf{w} \to \sqrt{\mathbf{w}}$ in (19.3) does *not* yield a polynomial hodograph when applied to a general polynomial hodograph — in fact, it will give a polynomial hodograph only when applied to a *Pythagorean* hodograph. Thus, regarding P and its inverse P^{-1} as mappings between sets of *polynomial* curves, we have $P(\Pi) = \hat{\Pi}$ and $P^{-1}(\hat{\Pi}) = \Pi$.

We call a regular polynomial curve $\mathbf{r}(t)$ and a regular PH curve $\hat{\mathbf{r}}(t)$ a pair of *corresponding curves* if they are mapped into each other under the action of P and P^{-1}. Such pairs can be expressed explicitly as

$$\begin{aligned} \mathbf{r}(t) \;&=\; \int_0^t u(\tau)\,\mathrm{d}\tau \;+\; \mathrm{i}\int_0^t v(\tau)\,\mathrm{d}\tau\,, \\ \hat{\mathbf{r}}(t) \;&=\; \int_0^t u^2(\tau) - v^2(\tau)\,\mathrm{d}\tau \;+\; \mathrm{i}\int_0^t 2\,u(\tau)v(\tau)\,\mathrm{d}\tau\,, \end{aligned} \tag{19.4}$$

where $u(t)$ and $v(t)$ are relatively prime polynomials, and we assume $\mathbf{r}(0) = \hat{\mathbf{r}}(0) = 0$ to fix translational freedoms.

Remark 19.1 The set $\hat{\Pi}$ of regular PH curves has the same "cardinality" or "power" as the set Π of regular polynomial curves.

The *cardinality* or *power* of an infinite set is a measure of its "size" [230] — specifically, two infinite sets have the same cardinality if we can establish a one–to–one correspondence between their members. Thus, in accordance with Proposition 19.1, we may say that there are "just as many" regular PH curves as there are regular polynomial curves in general.

Remark 19.2 The correspondence between the curves (19.4) refers not only to their geometrical loci, but also to the variation of the parameter t along those loci. Any polynomial curve $\mathbf{r}(t)$ may be re–parameterized by a linear transformation $t \to a + b\,t$ $(b \neq 0)$ without altering its geometrical locus, its regularity, or its degree. However, if $\mathbf{r}(t)$ and $\hat{\mathbf{r}}(t)$ are corresponding curves, re–parameterizing the former does not simply yield a new parameterization of the latter as the corresponding PH curve. Fixing translational freedoms by always placing the point of zero parameter value at the origin, it is not difficult to verify that the sequence of PH curves corresponding to all linear re–parameterizations of a given curve $\mathbf{r}(t)$ are actually *uniform scalings* of a unique curve $\hat{\mathbf{r}}(t)$ by the factor b (see Fig. 19.1).

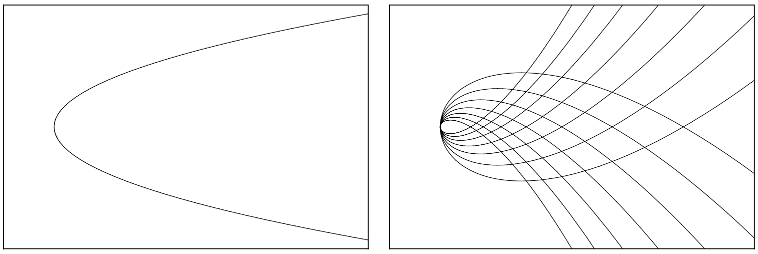

Fig. 19.1. Different parameterizations of a parabola (left) yield different scalings of a Tschirnhaus cubic (right) under the one–to–one correspondence of Proposition 19.1.

Now all linear re–parameterizations of a given PH curve are clearly also PH curves. Thus, if $\hat{\Pi}_\star$ is a subset of the space $\hat{\Pi}$ of regular PH curves whose members are simply the various (fixed–degree) parameterizations of a unique locus, it follows from Remark 19.2 that the pre–image $\Pi_\star = P^{-1}(\hat{\Pi}_\star)$ of $\hat{\Pi}_\star$ under the map P consists of *polynomial curves with mutually distinct loci.*

Example 19.1 The PH curve corresponding to the parabola $\mathbf{r}_1(t) = t + \mathrm{i}\,t^2$ is the Tschirnhaus cubic $\hat{\mathbf{r}}_1(t) = t - \frac{4}{3}\,t^3 + \mathrm{i}\,2t^2$. Consider now the sequence of parabolae $\mathbf{r}_k(t) = kt + \mathrm{i}\,k^3t^2$ for $0 < k < \infty$, any two members $k_1 \neq k_2$ of which are clearly of different shape. The PH curve corresponding to member k is easily verified to be $\hat{\mathbf{r}}_k(t) = k^2t - \frac{4}{3}\,k^6t^3 + \mathrm{i}\,2k^4t^2$. By setting $t = \tau/k^2$, however, we observe that $\hat{\mathbf{r}}_k(t) \equiv \hat{\mathbf{r}}_1(\tau)$ for all k. Thus, P maps the family of geometrically distinct parabolae $\mathbf{r}_k(t)$ into the different parameterizations of a geometrically unique cubic, $\hat{\mathbf{r}}_1(t)$ — see Fig. 19.2.

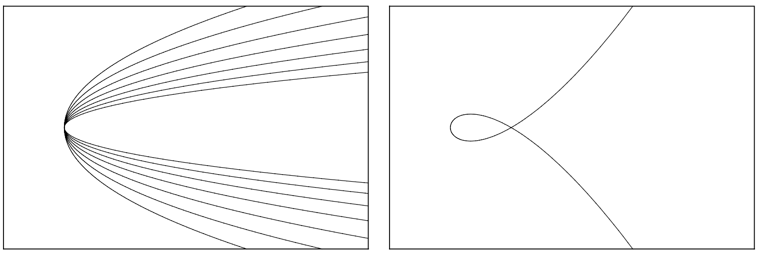

Fig. 19.2. Parabolas of different shape (left) yield different parameterizations of a Tschirnhaus cubic (right) under the one–to–one correspondence of Proposition 19.1.

Lemma 19.1 *The degrees n and $\hat{n}$ of corresponding curves $\mathbf{r}(t)$ and $\hat{\mathbf{r}}(t)$ are related by $\hat{n} = 2n - 1$.*

Proof : Let $u(t)$ and $v(t)$ be two relatively prime polynomials, and let $m = \max(\deg(u), \deg(v))$. Integrating the hodograph $\mathbf{w}(t) = u(t) + \mathrm{i}\,v(t)$ then gives a polynomial curve $\mathbf{r}(t)$ of degree $n = m + 1$. Further, one can easily verify that $\max(\deg(u^2 - v^2), \deg(2uv)) = 2m$, so integrating $\hat{\mathbf{w}}(t) = u^2(t) - v^2(t) + \mathrm{i}\, 2u(t)v(t)$ gives a PH curve $\hat{\mathbf{r}}(t)$ of degree $\hat{n} = 2m + 1 = 2n - 1$. ∎

Clearly, there are no *regular* PH curves of even degree. Straight lines in Π correspond to (different) straight lines in $\hat{\Pi}$, but P maps regular polynomial curves of degree ≥ 2 to regular PH curves of higher *odd* degree (see Table 19.1).

Table 19.1. Corresponding curves of low degree.

	polynomial curve $\mathbf{r}(t)$	PH curve $\hat{\mathbf{r}}(t)$
$n = 1$	straight lines	straight lines
$n = 2$	parabolae	Tschirnhaus cubics
$n = 3$	regular cubics	regular PH quintics
...	...	...

The properties of the map $\mathbf{w} \to \hat{\mathbf{w}} = \mathbf{w}^2$ are described in most textbooks on complex analysis — see, for example, [42, pp. 79–84]. As is well known [196] it takes the *Gaussian integers* or "grid points" $\alpha + \mathrm{i}\,\beta$ (where $\alpha, \beta \in \mathbb{Z}$) of the complex plane into points $\alpha^2 - \beta^2 + \mathrm{i}\, 2\alpha\beta$ whose real and imaginary parts are members of *integer Pythagorean triples.* The map is conformal everywhere except $\mathbf{w} = 0$; this exceptional point need not concern us if we consider only regular curves. Note also that it gives a *double covering* of the complex plane, each point $\hat{\mathbf{w}}$ having two pre–images, $-\mathbf{w}$ and $+\mathbf{w}$. Writing $\mathbf{w} = u + \mathrm{i}\, v$ and $\hat{\mathbf{w}} = \hat{u} + \mathrm{i}\,\hat{v}$, the pre–images of the grid lines $\hat{u} =$ constant and $\hat{v} =$ constant of the $\hat{\mathbf{w}}$ plane are, respectively, the families of rectangular hyperbolae

$$u^2 - v^2 \,=\, \hat{u} \qquad \text{and} \qquad 2uv \,=\, \hat{v}$$

in the $\mathbf{w}$ plane, with asymptotes $u = \pm v$ and $u = 0$, $v = 0$. On the other hand, the grid lines $u =$ constant and $v =$ constant of the $\mathbf{w}$ plane are respectively mapped into the families of confocal parabolae

$$\hat{v}^2 + 4u^2\hat{u} \,=\, 4u^4 \qquad \text{and} \qquad \hat{v}^2 - 4v^2\hat{u} \,=\, 4v^4$$

in the $\hat{\mathbf{w}}$ plane, whose vertices lie along the positive and negative $\hat{u}$–axis. In the limits $u \to 0$ and $v \to 0$, we obtain the half–lines $\hat{u} < 0$ and $\hat{u} > 0$, doubly traced, as images of the imaginary and real axes (see Fig. 19.3).

In terms of the velocity vector $\mathbf{w}(t) = \mathbf{r}'(t) = \sigma(t)\,\mathrm{e}^{\mathrm{i}\psi(t)}$ at each point of a given curve $\mathbf{r}(t)$, describing motion with speed $\sigma(t)$ at an angle $\psi(t)$ relative to the real axis, the map $\mathbf{w} \to \mathbf{w}^2$ transforms this velocity (see Fig. 19.3) by *squaring* the speed and *doubling* the inclination angle,

$$\hat{\sigma}(t) \,=\, \sigma^2(t) \qquad \text{and} \qquad \hat{\psi}(t) \,=\, 2\,\psi(t)\,.$$

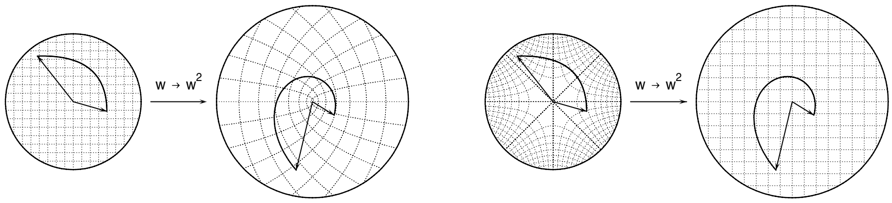

Fig. 19.3. The map $\mathbf{w} \to \hat{\mathbf{w}} = \mathbf{w}^2$ of the hodograph plane squares the lengths of velocity vectors and doubles their inclination angles. Left: grid lines in the $\mathbf{w}$ plane are mapped to families of confocal parabolae in the $\hat{\mathbf{w}}$ plane. Right: the pre–images of grid lines in the $\hat{\mathbf{w}}$ plane are families of rectangular hyperbolae in the $\mathbf{w}$ plane.

Proposition 19.2 *The control points of a regular PH curve of degree $2n-1$ are given in terms of n complex values $\mathbf{w}_0, \ldots, \mathbf{w}_{n-1}$ by the recursive formula*

$$\mathbf{p}_{k+1} = \mathbf{p}_k + \frac{1}{2n-1} \sum_{j=\max(0,k-n+1)}^{\min(k,n-1)} \frac{\binom{n-1}{j}\binom{n-1}{k-j}}{\binom{2n-2}{k}} \mathbf{w}_j \mathbf{w}_{k-j} \tag{19.5}$$

for $k = 0, 1, \ldots, 2n-2$, where $\mathbf{p}_0$ is arbitrary and $\mathbf{w}_0, \ldots, \mathbf{w}_{n-1}$ are such that the hodograph $\mathbf{w}(t)$ defined by (19.2) *does not traverse the origin.*

Proof : The square of the complex hodograph (19.2) may be written as

$$\hat{\mathbf{w}}(t) = \sum_{k=0}^{2n-2} \hat{\mathbf{w}}_k \binom{2n-2}{k} (1-t)^{2n-2-k} t^k \tag{19.6}$$

where, making use of the product rule (11.20) for Bernstein–form polynomials, the coefficients $\hat{\mathbf{w}}_k$ are given in terms of $\mathbf{w}_0, \ldots, \mathbf{w}_{n-1}$ by

$$\hat{\mathbf{w}}_k = \sum_{j=\max(0,k-n+1)}^{\min(k,n-1)} \frac{\binom{n-1}{j}\binom{n-1}{k-j}}{\binom{2n-2}{k}} \mathbf{w}_j \mathbf{w}_{k-j}\,, \quad k = 0, \ldots, 2n-2\,.$$

To integrate the hodograph (19.6), we employ property (11.7) of the Bernstein basis functions. This yields the quoted form (19.5) for the control points of a PH curve of degree $2n-1$, with an arbitrary constant of integration $\mathbf{p}_0$. ■

The requirement that the hodograph (19.2) defined by $\mathbf{w}_0, \ldots, \mathbf{w}_{n-1}$ must not pass through the origin for the control points (19.5) to define a *regular* PH curve does not, in general, have an intuitive geometrical interpretation in terms of the locations of $\mathbf{w}_0, \ldots, \mathbf{w}_{n-1}$. This requirement amounts to the gcd of the real and imaginary parts of (19.2), $u(t)$ and $v(t)$, being a constant — or to their resultant with respect to t being non–zero. Criteria specific to the PH cubics and quintics are given in equations (19.10) and (19.13) below.

19.3 Rotation Invariance of Hodographs

The complex representation offers a simple proof for the *rotation invariance* of the sufficient–and–necessary form

$$x'(t) \,=\, u^2(t) - v^2(t)\,, \quad y'(t) \,=\, 2u(t)v(t)\,, \quad \sigma(t) \,=\, u^2(t) + v^2(t)$$

for primitive planar Pythagorean hodographs $\mathbf{r}'(t) = (x'(t), y'(t))$ satisfying

$$x'^2(t) \,+\, y'^2(t) \,=\, \sigma^2(t)\,,$$

where $\gcd(u,v) = \text{constant} \Rightarrow \gcd(x',y') = \text{constant}$. On making a rotation

$$\begin{bmatrix} \tilde{x}'(t) \\ \tilde{y}'(t) \end{bmatrix} \,=\, \begin{bmatrix} \cos\theta & -\sin\theta \\ \sin\theta & \cos\theta \end{bmatrix} \begin{bmatrix} x'(t) \\ y'(t) \end{bmatrix}$$

through angle θ, we seek to express the rotated hodograph $\tilde{\mathbf{r}}'(t) = (\tilde{x}'(t), \tilde{y}'(t))$ in terms of two new polynomials $\tilde{u}(t)$, $\tilde{v}(t)$ as

$$\tilde{x}'(t) \,=\, \tilde{u}^2(t) - \tilde{v}^2(t)\,, \quad \tilde{y}'(t) \,=\, 2\tilde{u}(t)\tilde{v}(t)\,. \tag{19.7}$$

One can easily see that the transformed hodograph,

$$\begin{aligned} \tilde{x}'(t) \,&=\, \cos\theta\,[\,u^2(t) - v^2(t)\,] \,-\, \sin\theta\,2u(t)v(t)\,, \\ \tilde{y}'(t) \,&=\, \sin\theta\,[\,u^2(t) - v^2(t)\,] \,+\, \cos\theta\,2u(t)v(t)\,, \end{aligned}$$

is obtained by substituting into (19.7) the polynomials

$$\tilde{u}(t) \,=\, \cos\tfrac{1}{2}\theta\,u(t) - \sin\tfrac{1}{2}\theta\,v(t)\,, \quad \tilde{v}(t) \,=\, \sin\tfrac{1}{2}\theta\,u(t) + \cos\tfrac{1}{2}\theta\,v(t)\,. \tag{19.8}$$

Using the complex representation $\mathbf{r}'(t) = \mathbf{w}^2(t)$ where $\mathbf{w}(t) = u(t) + \mathrm{i}\,v(t)$, the rotation yields $\tilde{\mathbf{r}}'(t) = \exp(\mathrm{i}\,\theta)\,\mathbf{w}^2(t) = \tilde{\mathbf{r}}'(t) = \tilde{\mathbf{w}}^2(t)$, the real and imaginary parts of $\tilde{\mathbf{w}}(t) = \exp(\mathrm{i}\tfrac{1}{2}\theta)\,\mathbf{w}(t) = \tilde{u}(t) + \mathrm{i}\,\tilde{v}(t)$ being defined by (19.8).

19.4 Pythagorean–hodograph Cubics Revisited

In the first non–trivial instance, that of the PH cubics, expression (19.5) yields control points of the form

$$\mathbf{p}_1 \,=\, \mathbf{p}_0 + \frac{1}{3}\,\mathbf{w}_0^2\,, \quad \mathbf{p}_2 \,=\, \mathbf{p}_1 + \frac{1}{3}\,\mathbf{w}_0\mathbf{w}_1\,, \quad \mathbf{p}_3 \,=\, \mathbf{p}_2 + \frac{1}{3}\,\mathbf{w}_1^2\,. \tag{19.9}$$

Here, the complex values $\mathbf{w}_0$ and $\mathbf{w}_1$ must satisfy

$$\mathrm{Im}(\overline{\mathbf{w}}_0\mathbf{w}_1) \neq 0 \tag{19.10}$$

to obtain a regular curve. If $\mathbf{w}_0 = u_0 + \mathrm{i}\,v_0$ and $\mathbf{w}_1 = u_1 + \mathrm{i}\,v_1$, this amounts to $u_0v_1 \neq u_1v_0$ — i.e., the line from $\mathbf{w}_0$ to $\mathbf{w}_1$ should not pass through the origin.

The complex form offers a succinct expression of the sufficient–and–necessary conditions (18.6) characterizing PH cubics by the control–polygon geometry. Writing equations (19.9) in terms of the control–polygon legs as

$$3\Delta\mathbf{p}_0 \,=\, \mathbf{w}_0^2\,, \qquad 3\Delta\mathbf{p}_1 \,=\, \mathbf{w}_0\mathbf{w}_1\,, \qquad 3\Delta\mathbf{p}_2 \,=\, \mathbf{w}_1^2\,,$$

we may eliminate $\mathbf{w}_0$ and $\mathbf{w}_1$ to obtain the single complex constraint

$$(\Delta\mathbf{p}_1)^2 \,=\, \Delta\mathbf{p}_2\Delta\mathbf{p}_0\,, \tag{19.11}$$

whose satisfaction distinguishes the PH cubics from "ordinary" cubics. To see that the complex constraint (19.11) is equivalent to the two real constraints (18.6), we write the directed control–polygon legs in polar form as

$$\Delta\mathbf{p}_0 \,=\, L_0\,\mathrm{e}^{\,\mathrm{i}\xi_0}\,, \qquad \Delta\mathbf{p}_1 \,=\, L_1\,\mathrm{e}^{\,\mathrm{i}\xi_1}\,, \qquad \Delta\mathbf{p}_2 \,=\, L_2\,\mathrm{e}^{\,\mathrm{i}\xi_2}\,.$$

Substituting into (19.11), we obtain $L_1^2 = L_2L_0$ and $2\xi_1 = \xi_0 + \xi_2$. In terms of the control polygon interior angles, $\theta_1 = \pi + \xi_1 - \xi_0$ and $\theta_2 = \pi + \xi_2 - \xi_1$, the latter condition implies that $\theta_2 = \theta_1$. Clearly, this derivation[3] is much simpler than that given in §18.3 using only real variables.

We may regard general cubics as possessing eight degrees of freedom (the coordinates of their control points), although not all of them are intrinsic shape freedoms. Each cubic can be regarded as a point in a Euclidean space $\mathbb{R}^8$ with coordinates $(x_0, y_0, x_1, y_1, x_2, y_2, x_3, y_3)$, and the real and imaginary parts of (19.11) each define a degree 2 hypersurface (a *hyperquadric*) in this space. PH cubics lie on the intersection of the hyperquadrics, a locus of dimension 6.

19.5 Characterization of the PH Quintics

The PH quintics are of great practical interest, since they are the simplest PH curves that may inflect, and match first–order Hermite data (see Chap. 25). For regular curves, there is a unique correspondence between PH quintics and ordinary cubics, so we may expect similar "shape flexibility" among these two sets of curves. The control points (19.5) for PH quintics are of the form

$$\begin{aligned}
\mathbf{p}_1 \,&=\, \mathbf{p}_0 + \frac{1}{5}\,\mathbf{w}_0^2\,, \\
\mathbf{p}_2 \,&=\, \mathbf{p}_1 + \frac{1}{5}\,\mathbf{w}_0\mathbf{w}_1\,, \\
\mathbf{p}_3 \,&=\, \mathbf{p}_2 + \frac{1}{5}\,\frac{2\mathbf{w}_1^2 + \mathbf{w}_0\mathbf{w}_2}{3}\,, \\
\mathbf{p}_4 \,&=\, \mathbf{p}_3 + \frac{1}{5}\,\mathbf{w}_1\mathbf{w}_2\,, \\
\mathbf{p}_5 \,&=\, \mathbf{p}_4 + \frac{1}{5}\,\mathbf{w}_2^2\,.
\end{aligned} \tag{19.12}$$

[3] The possibility of such a derivation was first noted by Professor Wendelin Degen.

Comparing (17.6) with (19.12) illustrates the economy of expression afforded by the complex representation. The constraint that ensures regularity of the PH curve defined by (19.12) may be written in the form

$$[\,\mathrm{Im}(\overline{\mathbf{w}}_0\mathbf{w}_2)\,]^2 \;-\; 4\,\mathrm{Im}(\overline{\mathbf{w}}_0\mathbf{w}_1)\,\mathrm{Im}(\overline{\mathbf{w}}_1\mathbf{w}_2) \;\neq\; 0\,, \tag{19.13}$$

or explicitly in terms of the real and imaginary parts of $\mathbf{w}_0, \mathbf{w}_1, \mathbf{w}_2$ as

$$(u_0v_2 - u_2v_0)^2 \;\neq\; 4\,(u_0v_1 - u_1v_0)\,(u_1v_2 - u_2v_1)\,. \tag{19.14}$$

Although (19.13) does not have an intuitive geometrical meaning, we note as an immediate consequence that $\mathbf{w}_0$ and $\mathbf{w}_2$ must be non–zero, i.e., $\mathbf{p}_0 \neq \mathbf{p}_1$ and $\mathbf{p}_4 \neq \mathbf{p}_5$ (otherwise the parametric speed is zero at $t = 0$ or 1).

We now use the complex form to derive a characterization for PH quintics in terms of the control polygon geometry. We begin by re–writing equations (19.12) in terms of the directed control polygon legs $\Delta\mathbf{p}_k = \mathbf{p}_{k+1} - \mathbf{p}_k$ as

$$\begin{aligned}
\Delta\mathbf{p}_0 &= \frac{\mathbf{w}_0^2}{5}\,, \quad \Delta\mathbf{p}_1 \;=\; \frac{\mathbf{w}_0\mathbf{w}_1}{5}\,, \\
\Delta\mathbf{p}_2 &= \frac{2\mathbf{w}_1^2 + \mathbf{w}_0\mathbf{w}_2}{15}\,, \\
\Delta\mathbf{p}_3 &= \frac{\mathbf{w}_1\mathbf{w}_2}{5}\,, \quad \Delta\mathbf{p}_4 \;=\; \frac{\mathbf{w}_2^2}{5}\,.
\end{aligned} \tag{19.15}$$

It is understood that, for a regular curve, $\Delta\mathbf{p}_0 \neq 0$ and $\Delta\mathbf{p}_4 \neq 0$.

Proposition 19.3 *Let the control–polygon legs of a regular quintic be defined by complex values $\Delta\mathbf{p}_0, \ldots, \Delta\mathbf{p}_4$. Then the curve has a Pythagorean hodograph if and only if these values satisfy*

$$\Delta\mathbf{p}_0(\Delta\mathbf{p}_3)^2 \;=\; \Delta\mathbf{p}_4(\Delta\mathbf{p}_1)^2\,, \tag{19.16}$$

and are consistent with the following system of constraints:

$$\begin{aligned}
3\,\Delta\mathbf{p}_0\Delta\mathbf{p}_1\Delta\mathbf{p}_2 - (\Delta\mathbf{p}_0)^2\Delta\mathbf{p}_3 - 2\,(\Delta\mathbf{p}_1)^3 &= 0\,, \\
3\,\Delta\mathbf{p}_4\Delta\mathbf{p}_3\Delta\mathbf{p}_2 - (\Delta\mathbf{p}_4)^2\Delta\mathbf{p}_1 - 2\,(\Delta\mathbf{p}_3)^3 &= 0\,, \\
3\,\Delta\mathbf{p}_0\Delta\mathbf{p}_3\Delta\mathbf{p}_2 - \Delta\mathbf{p}_4\Delta\mathbf{p}_0\Delta\mathbf{p}_1 - 2\,(\Delta\mathbf{p}_1)^2\Delta\mathbf{p}_3 &= 0\,, \\
3\,\Delta\mathbf{p}_4\Delta\mathbf{p}_1\Delta\mathbf{p}_2 - \Delta\mathbf{p}_0\Delta\mathbf{p}_4\Delta\mathbf{p}_3 - 2\,(\Delta\mathbf{p}_3)^2\Delta\mathbf{p}_1 &= 0\,, \\
9\,\Delta\mathbf{p}_0(\Delta\mathbf{p}_2)^2 - 6\,(\Delta\mathbf{p}_1)^2\Delta\mathbf{p}_2 - 2\,\Delta\mathbf{p}_0\Delta\mathbf{p}_1\Delta\mathbf{p}_3 - (\Delta\mathbf{p}_0)^2\Delta\mathbf{p}_4 &= 0\,, \\
9\,\Delta\mathbf{p}_4(\Delta\mathbf{p}_2)^2 - 6\,(\Delta\mathbf{p}_3)^2\Delta\mathbf{p}_2 - 2\,\Delta\mathbf{p}_4\Delta\mathbf{p}_3\Delta\mathbf{p}_1 - (\Delta\mathbf{p}_4)^2\Delta\mathbf{p}_0 &= 0\,.
\end{aligned} \tag{19.17}$$

Before proceeding with the proof, some explanatory remarks are in order. Ordinarily, when $\Delta\mathbf{p}_1$ and $\Delta\mathbf{p}_3$ are both non–zero, equation (19.16) and *one* of the first four of equations (19.17) define sufficient–and–necessary conditions for a quintic to be a PH curve. If $\Delta\mathbf{p}_1 = \Delta\mathbf{p}_3 = 0$, however, (19.16) and the first four equations in (19.17) become identities, and we must take (a simplified form of) *either* of the last two of equations (19.17) as such a condition.

Proof of Proposition 19.3 : The necessity of *all* of the conditions in (19.16) and (19.17) follows from eliminating $\mathbf{w}_0, \mathbf{w}_1, \mathbf{w}_2$ from equations (19.15). For example, if we assume $\Delta\mathbf{p}_0, \ldots, \Delta\mathbf{p}_4$ are of the form (19.15), we see from the first and last of these equations that $\mathbf{w}_0^2 : \mathbf{w}_2^2 = \Delta\mathbf{p}_0 : \Delta\mathbf{p}_4$, while from the second and fourth we have $\mathbf{w}_0 : \mathbf{w}_2 = \Delta\mathbf{p}_1 : \Delta\mathbf{p}_3$. From these expressions it is evident that condition (19.16) must be satisfied. Likewise, the necessity of the six conditions (19.17) is verified by substituting directly from (19.15).

Concerning the sufficiency of the stated conditions, we need to show that if equations (19.16) and (19.17) are satisfied, then $\Delta\mathbf{p}_0, \ldots, \Delta\mathbf{p}_4$ must be of the form (19.15). Consider first equation (19.16). Without loss of generality, we may write $\Delta\mathbf{p}_0 = \mathbf{a}^2$ and $\Delta\mathbf{p}_4 = \mathbf{c}^2$ where, as noted above, $\mathbf{a}$ and $\mathbf{c}$ are *non–zero* complex numbers for a regular curve. Equation (19.16) then becomes

$$\mathbf{a}^2\,(\Delta\mathbf{p}_3)^2 \;=\; \mathbf{c}^2\,(\Delta\mathbf{p}_1)^2\,,$$

and if $\Delta\mathbf{p}_1$ and $\Delta\mathbf{p}_3$ are to satisfy the above, they must be of the form

$$\Delta\mathbf{p}_1 \;=\; \mathbf{ab} \qquad \text{and} \qquad \Delta\mathbf{p}_3 \;=\; \mathbf{bc}$$

for some complex number $\mathbf{b}$ (not necessarily non–zero).

With these results, we may regard the six equations (19.17) as defining the value of $\Delta\mathbf{p}_2$. Specifically, on substituting into (19.17) we obtain

$$\begin{aligned}
\mathbf{a}^3\mathbf{b}\,\left[\,3\,\Delta\mathbf{p}_2 \,-\, \mathbf{ac} \,-\, 2\,\mathbf{b}^2\,\right] &= 0\,,\\
\mathbf{bc}^3\,\left[\,3\,\Delta\mathbf{p}_2 \,-\, \mathbf{ac} \,-\, 2\,\mathbf{b}^2\,\right] &= 0\,,\\
\mathbf{a}^2\mathbf{bc}\,\left[\,3\,\Delta\mathbf{p}_2 \,-\, \mathbf{ac} \,-\, 2\,\mathbf{b}^2\,\right] &= 0\,,\\
\mathbf{abc}^2\,\left[\,3\,\Delta\mathbf{p}_2 \,-\, \mathbf{ac} \,-\, 2\,\mathbf{b}^2\,\right] &= 0\,,\\
\mathbf{a}^2\,\left[\,9\,(\Delta\mathbf{p}_2)^2 \,-\, 6\,\mathbf{b}^2\Delta\mathbf{p}_2 \,-\, 2\,\mathbf{ab}^2\mathbf{c} \,-\, \mathbf{a}^2\mathbf{c}^2\,\right] &= 0\,,\\
\mathbf{c}^2\,\left[\,9\,(\Delta\mathbf{p}_2)^2 \,-\, 6\,\mathbf{b}^2\Delta\mathbf{p}_2 \,-\, 2\,\mathbf{ab}^2\mathbf{c} \,-\, \mathbf{a}^2\mathbf{c}^2\,\right] &= 0\,,
\end{aligned}$$

and we must distinguish two cases, according to the value of $\mathbf{b}$.

Case (i) $\mathbf{b} \neq 0$: The first four equations above are obviously equivalent and yield the same solution

$$\Delta\mathbf{p}_2 \;=\; \frac{2\mathbf{b}^2 + \mathbf{ac}}{3}\,,$$

for $\Delta\mathbf{p}_2$. The last two equations, on the other hand, give

$$\Delta\mathbf{p}_2 \;=\; \frac{2\mathbf{b}^2 + \mathbf{ac}}{3} \quad \text{or} \quad -\,\frac{\mathbf{ac}}{3}\,, \tag{19.18}$$

but the second solution must be discarded, since if $\mathbf{b} \neq 0$ it is inconsistent with the first four equations. Thus, equations (19.16) and (19.17) imply that $\Delta\mathbf{p}_0, \ldots, \Delta\mathbf{p}_4$ can be expressed as

$$\Delta\mathbf{p}_0 = \mathbf{a}^2, \quad \Delta\mathbf{p}_1 = \mathbf{ab}, \quad \Delta\mathbf{p}_2 = \frac{2\mathbf{b}^2 + \mathbf{ac}}{3}, \quad \Delta\mathbf{p}_3 = \mathbf{bc}, \quad \Delta\mathbf{p}_4 = \mathbf{c}^2$$

which is clearly of the form (19.15) with $(\mathbf{w}_0, \mathbf{w}_1, \mathbf{w}_2) = \sqrt{5}\,(\mathbf{a}, \mathbf{b}, \mathbf{c})$.

Case (ii) $\mathbf{b} = 0$: The first four of equations (19.17) degenerate to identities and yield no information concerning $\Delta\mathbf{p}_2$, whereas the last two both simplify to $9\,(\Delta\mathbf{p}_2)^2 - \mathbf{a}^2\mathbf{c}^2 = 0$, giving solutions

$$\Delta\mathbf{p}_2 \;=\; \pm\,\frac{\mathbf{ac}}{3}$$

that correspond to expressions (19.18) with $\mathbf{b} = 0$. Hence we have

$$\Delta\mathbf{p}_0 = \mathbf{a}^2, \quad \Delta\mathbf{p}_1 = 0, \quad \Delta\mathbf{p}_2 = \pm\,\frac{\mathbf{ac}}{3}, \quad \Delta\mathbf{p}_3 = 0, \quad \Delta\mathbf{p}_4 = \mathbf{c}^2$$

which is also of the form (19.15), with $(\mathbf{w}_0, \mathbf{w}_1, \mathbf{w}_2) = \sqrt{5}\,(\pm\mathbf{a}, 0, \pm\mathbf{c})$. ∎

Equations (19.16) and (19.17) were obtained by a Gröbner basis reduction on the system (19.15), employing a lexical ordering with $\mathbf{w}_0, \mathbf{w}_1, \mathbf{w}_2$ preceding $\Delta\mathbf{p}_0, \ldots, \Delta\mathbf{p}_4$. Expressions (19.16) and (19.17) comprise all elements of the basis that do not depend on $\mathbf{w}_0, \mathbf{w}_1, \mathbf{w}_2$. We distinguish (19.16) from the other conditions (19.17) since: (i) it has a simple geometrical interpretation — see Remark 19.3; and (ii) among (19.16) and (19.17), it is the only condition that is *individually* invariant under reverse–ordering of the control–polygon legs. The significance of the latter point is that the substitution

$$\Delta\mathbf{p}_k \;\to\; -\,\Delta\mathbf{p}_{4-k} \qquad k = 0, \ldots, 4 \tag{19.19}$$

amounts to the re–parameterization $t \to 1 - t$, under which the Pythagorean nature of the hodograph must be preserved. While (19.16) is clearly unaltered by the substitution (19.19), the *individual* members of the system (19.17) are not (the entire system is invariant, however — the equations are grouped into pairs whose members clearly map into each other under (19.19)).

Additional necessary control–polygon constraints can be derived, that are symmetric with respect to the labelling of its legs. The quartic condition

$$9\,(\Delta\mathbf{p}_2)^2\Delta\mathbf{p}_0\Delta\mathbf{p}_4 \;=\; [\,2\,\Delta\mathbf{p}_1\Delta\mathbf{p}_3 + \Delta\mathbf{p}_0\Delta\mathbf{p}_4\,]^2\,, \tag{19.20}$$

for example, follows straightforwardly from expressions (19.15). In conjunction with (19.16), however, this does not amount to a *sufficient* condition for a PH curve, since if we choose $\Delta\mathbf{p}_0 = \mathbf{a}^2$, $\Delta\mathbf{p}_1 = \mathbf{ab}$, $\Delta\mathbf{p}_3 = \mathbf{bc}$, $\Delta\mathbf{p}_4 = \mathbf{c}^2$ then equation (19.20) gives two possibilities for the middle leg

$$\Delta\mathbf{p}_2 \;=\; \pm\,\frac{2\mathbf{b}^2 + \mathbf{ac}}{3}\,,$$

of which only the *positive* sign choice yields a Pythagorean hodograph.

Regarding quintics as residing in a 12–dimensional space defined by their control–point coordinates, the real and imaginary parts of equation (19.16) and of any one of the equations (19.17) define four cubic hypersurfaces in this space, on whose intersection — a locus of apparent dimension eight — the PH quintics lie (not all these dimensions correspond to intrinsic shape freedoms).

19.6 Geometry of the Control Polygon

As noted above, it is usually possible to take condition (19.16) and just *one* of the first four of conditions (19.17) as characterizing the PH quintics. We quote the entire system for completeness, and to highlight symmetry properties.

Remark 19.3 Condition (19.16) admits a simple geometrical interpretation. Expressing the control polygon legs in polar form $\Delta\mathbf{p}_k = L_k \mathrm{e}^{\,\mathrm{i}\xi_k}$, $k = 0,\ldots,4$ immediately gives $L_0 L_3^2 = L_4 L_1^2$ and $\xi_0 + 2\xi_3 = \xi_4 + 2\xi_1$. Re–phrasing the latter in terms of the four "interior" angles $\theta_i = \pi + \xi_i - \xi_{i-1}$ for $i = 1,\ldots,4$ we see that the geometry of the control polygon is constrained by the relations

$$\frac{L_1}{L_3} = \sqrt{\frac{L_0}{L_4}} \qquad \text{and} \qquad \theta_1 + \theta_4 = \theta_2 + \theta_3 \,. \tag{19.21}$$

The remaining conditions (19.17) do not have geometrical interpretations as intuitive as (19.21). Assuming that $\Delta\mathbf{p}_0,\ldots,\Delta\mathbf{p}_4 \neq 0$ we focus on the first of equations (19.17). Substituting $\Delta\mathbf{p}_k = L_k \mathrm{e}^{\,\mathrm{i}\xi_k}$ and $\theta_i = \pi + \xi_i - \xi_{i-1}$ as before, we obtain the equation

$$3\,L_0 L_1 L_2\,\mathrm{e}^{\,\mathrm{i}(2\theta_1+\theta_2)} \,-\, L_0^2 L_3\,\mathrm{e}^{\,\mathrm{i}(\theta_1+\theta_2+\theta_3)} \,-\, 2\,L_1^3\,\mathrm{e}^{\,\mathrm{i}3\theta_1} \,=\, 0\,.$$

This can be further simplified upon dividing by $\mathrm{e}^{\,\mathrm{i}2\theta_1}$ and using (19.21) to set $\theta_2 + \theta_3 - \theta_1 = \theta_4$ in the middle term. Hence we have

$$3\,L_0 L_1 L_2\,\mathrm{e}^{\,\mathrm{i}\theta_2} \,-\, L_0^2 L_3\,\mathrm{e}^{\,\mathrm{i}\theta_4} \,-\, 2\,L_1^3\,\mathrm{e}^{\,\mathrm{i}\theta_1} \,=\, 0\,,$$

and the real and imaginary parts of this equation furnish two constraints

$$\begin{aligned} 3\,L_0 L_1 L_2 \cos\theta_2 \,&=\, L_0^2 L_3 \cos\theta_4 \,+\, 2\,L_1^3 \cos\theta_1\,, \\ 3\,L_0 L_1 L_2 \sin\theta_2 \,&=\, L_0^2 L_3 \sin\theta_4 \,+\, 2\,L_1^3 \sin\theta_1\,, \end{aligned} \tag{19.22}$$

which, together with (19.21), constitute sufficient and necessary conditions for a Pythagorean hodograph. Condition analogous to (19.22) result if we select instead the second, third, or fourth of the first four equations in (19.17).

Remark 19.4 The control polygons of PH quintics have *five* shape freedoms, since they are characterized by *four* constraints, equations (19.21) and (19.22), on the *nine* parameters $L_0,\ldots,L_4$ and $\theta_1,\ldots,\theta_4$. This is consistent with the fact that there are a finite number (four) of PH quintic solutions to the first–order Hermite interpolation problem, which corresponds to identifying PH quintics with specified control points $\mathbf{p}_0$, $\mathbf{p}_1$ and $\mathbf{p}_4$, $\mathbf{p}_5$. Fixing non–essential freedoms by taking $\mathbf{p}_0 = 0$ and $\mathbf{p}_1 = x_1$ (a real value), corresponding to a choice of the origin and orientation of the axes, this entails five free choices for the values $x_4 = \mathrm{Re}(\mathbf{p}_4)$, $y_4 = \mathrm{Im}(\mathbf{p}_4)$, $x_5 = \mathrm{Re}(\mathbf{p}_5)$, $y_5 = \mathrm{Im}(\mathbf{p}_5)$, and y_1. As these requirements match the intrinsic freedoms of PH quintics, the Hermite interpolants cannot depend on any free parameters (see Chap. 25).

Remark 19.5 The control polygons of PH quintics may be generated from two complex "shape parameters" $\boldsymbol{\sigma}$ and $\boldsymbol{\tau}$, as follows:

- take points $\boldsymbol{\zeta}_k = \boldsymbol{\sigma}^k$ for $k = -2, -1, 0, 1, 2$ on a logarithmic spiral through $\boldsymbol{\zeta}_0 = 1$, such that the angles between rays from the origin to these points are all equal, and set $\Delta\mathbf{p}_0 = \boldsymbol{\zeta}_{-2}$ and $\Delta\mathbf{p}_4 = \boldsymbol{\zeta}_2$;
- multiply $\boldsymbol{\zeta}_{-1}$ and $\boldsymbol{\zeta}_1$ by $\boldsymbol{\tau}$ to obtain $\Delta\mathbf{p}_1 = \boldsymbol{\tau}\boldsymbol{\zeta}_{-1}$ and $\Delta\mathbf{p}_3 = \boldsymbol{\tau}\boldsymbol{\zeta}_1$;
- and finally set $\Delta\mathbf{p}_2 = (2\boldsymbol{\tau}^2 + 1)\boldsymbol{\zeta}_0/3$.

This construction follows from the fact that multiplying the control polygon by any complex constant amounts to a *similarity transformation* — i.e., a scaling and rotation — under which its Pythagorean nature is preserved. In particular, expressions (19.15) are seen to be of the above form upon multiplying them by $(\mathbf{w}_0\mathbf{w}_2)^{-1}$ and taking $\boldsymbol{\sigma}^2 = \mathbf{w}_2/\mathbf{w}_0$ and $\boldsymbol{\tau}^2 = \mathbf{w}_1^2/(\mathbf{w}_0\mathbf{w}_2)$. Note that the constraints (19.21) follow directly from this construction.

The control points $\mathbf{p}_0, \ldots, \mathbf{p}_5$ of PH quintics are usually distinct: for *regular* PH quintics, in particular, it follows from (19.13) that $\mathbf{w}_0$ and $\mathbf{w}_2$ are non–zero, and thus $\mathbf{p}_0 \neq \mathbf{p}_1$ and $\mathbf{p}_4 \neq \mathbf{p}_5$. By appropriately choosing $\mathbf{w}_1$, however, it is possible to construct "degenerate" PH quintics that have coincident interior control points (see Fig. 19.4). These forms may be summarized as follows.

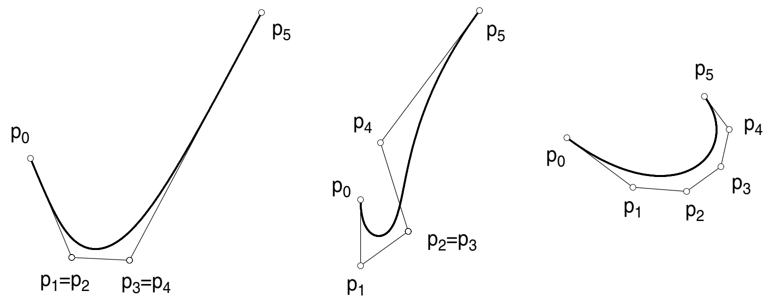

Fig. 19.4. Degenerate PH quintic control polygons — only 4 distinct control points (left); only 5 distinct control points (center); and a degree–elevated PH cubic (right).

Only Four Distinct Control Points

This case arises when we take $\mathbf{w}_1 = 0$ in (19.12), so that $\mathbf{p}_1 = \mathbf{p}_2$ and $\mathbf{p}_3 = \mathbf{p}_4$. The control polygon is then of the form

$$\Delta\mathbf{p}_0 = \frac{\mathbf{w}_0^2}{5}\,, \quad \Delta\mathbf{p}_1 = 0\,, \quad \Delta\mathbf{p}_2 = \pm\,\frac{\mathbf{w}_0\mathbf{w}_2}{15}\,, \quad \Delta\mathbf{p}_3 = 0\,, \quad \Delta\mathbf{p}_4 = \frac{\mathbf{w}_2^2}{5}\,.$$

Although there are only four distinct control points, this hodograph defines a true quintic PH, *not* a degree–elevated PH cubic (see below). Moreover, this curve is regular if $\mathbf{w}_0, \mathbf{w}_2 \neq 0$. As noted in the proof of Proposition 19.3, when

$\Delta\mathbf{p}_1 = \Delta\mathbf{p}_3 = 0$ the entire system of constraints (19.16) and (19.17) reduces to just $9\,(\Delta\mathbf{p}_2)^2 - \Delta\mathbf{p}_0\Delta\mathbf{p}_4 = 0$. Geometrically, this amounts to

$$3L_2 \,=\, \sqrt{L_0L_4} \qquad \text{and} \qquad \theta_a \,=\, \theta_b\,, \tag{19.23}$$

where L_0, L_2, L_4 are lengths of the non–zero control polygon legs, and θ_a, θ_b are the interior angles at $\mathbf{p}_1 = \mathbf{p}_2$ and $\mathbf{p}_3 = \mathbf{p}_4$. Conditions (19.23) are clearly reminiscent of the geometrical constraints (18.6) for PH cubics.

Only Five Distinct Control Points

In this case, the value of $\mathbf{w}_1$ is chosen such that $2\mathbf{w}_1^2 + \mathbf{w}_0\mathbf{w}_2 = 0$, and hence $\mathbf{p}_2 = \mathbf{p}_3$. Thus, $\Delta\mathbf{p}_2 = 0$ and the other control polygon legs can be expressed in terms of $\mathbf{w}_0$ and $\mathbf{w}_2$ only:

$$\Delta\mathbf{p}_0 = \frac{\mathbf{w}_0^2}{5}, \quad \Delta\mathbf{p}_1 = \pm\,\mathrm{i}\,\frac{\mathbf{w}_0}{5}\sqrt{\frac{\mathbf{w}_0\mathbf{w}_2}{2}}, \quad \Delta\mathbf{p}_3 = \pm\,\mathrm{i}\,\frac{\mathbf{w}_2}{5}\sqrt{\frac{\mathbf{w}_0\mathbf{w}_2}{2}}, \quad \Delta\mathbf{p}_4 = \frac{\mathbf{w}_2^2}{5}.$$

For this degenerate form, conditions (19.16) and (19.17) may be reduced to

$$\Delta\mathbf{p}_0(\Delta\mathbf{p}_3)^2 \,=\, \Delta\mathbf{p}_4(\Delta\mathbf{p}_1)^2 \qquad \text{and} \qquad \Delta\mathbf{p}_0\Delta\mathbf{p}_4 \,+\, 2\,\Delta\mathbf{p}_1\Delta\mathbf{p}_3 \,=\, 0\,.$$

In terms of the lengths L_0, L_1, L_3, L_4 of the control polygon legs and interior angles $\theta_a, \theta_b, \theta_c$ at $\mathbf{p}_1$, $\mathbf{p}_2 = \mathbf{p}_3$, $\mathbf{p}_4$, we obtain the geometrical constraints

$$\frac{L_1}{L_3} \,=\, \sqrt{\frac{L_0}{L_4}}\,, \quad \frac{L_0}{L_1} \,=\, 2\,\frac{L_3}{L_4}\,, \quad \theta_a - \theta_b + \theta_c \,=\, \pi\,, \quad \theta_a - \theta_c \,=\, \pm\pi\,.$$

Degree–elevated PH Cubics

It is possible to elevate the degree of any PH curve without compromising the Pythagorean nature of its hodograph, since degree elevation amounts merely to a redundant representation. Applying the degree elevation procedure (13.4) *twice* to the PH cubic control polygon (19.9) yields PH quintic control points

$$\begin{aligned}
\mathbf{p}_1 \,&=\, \mathbf{p}_0 + \frac{1}{5}\,\mathbf{w}_0^2\,, \\
\mathbf{p}_2 \,&=\, \mathbf{p}_1 + \frac{1}{10}\,(\mathbf{w}_0^2 + \mathbf{w}_0\mathbf{w}_1)\,, \\
\mathbf{p}_3 \,&=\, \mathbf{p}_2 + \frac{1}{30}\,(\mathbf{w}_0^2 + 4\mathbf{w}_0\mathbf{w}_1 + \mathbf{w}_1^2)\,, \\
\mathbf{p}_4 \,&=\, \mathbf{p}_3 + \frac{1}{10}\,(\mathbf{w}_0\mathbf{w}_1 + \mathbf{w}_1^2)\,, \\
\mathbf{p}_5 \,&=\, \mathbf{p}_4 + \frac{1}{5}\,\mathbf{w}_1^2\,.
\end{aligned} \tag{19.24}$$

One can verify that expressions (19.24) are of the form (19.12) with $\mathbf{w}_0, \mathbf{w}_1, \mathbf{w}_2$ replaced by $\mathbf{w}_0, \frac{1}{2}(\mathbf{w}_0 + \mathbf{w}_1), \mathbf{w}_1$. Thus, it follows that whenever the value $\mathbf{w}_1$ in equations (19.12) is the *mean* of the values $\mathbf{w}_0$ and $\mathbf{w}_2$, we have a PH cubic "masquerading" as a quintic, rather than a true PH quintic.

19.7 Intrinsic Features of Corresponding Curves

For a PH curve with complex hodograph $\mathbf{r}'(t) = \mathbf{w}^2(t)$, the parametric speed is evidently $\sigma(t) = |\mathbf{w}(t)|^2$. The unit tangent and normal may be expressed in terms of the complex polynomial $\mathbf{w}(t)$ as

$$\mathbf{t} \,=\, \mathbf{r}' \,/\, |\mathbf{r}'| \,=\, \mathbf{w} / \,\overline{\mathbf{w}} \qquad \text{and} \qquad \mathbf{n} \,=\, \mathbf{t} \times \mathbf{z} \,=\, \mathbf{w} /\, \mathrm{i}\, \overline{\mathbf{w}}\,, \tag{19.25}$$

while the curvature is given by

$$\kappa \,=\, \frac{1}{|\mathbf{r}'|}\, \mathrm{Im}\!\left(\frac{\mathbf{r}''}{\mathbf{r}'}\right) \,=\, \frac{\mathrm{Im}(\overline{\mathbf{r}}'\mathbf{r}'')}{|\mathbf{r}'|^3} \,=\, 2\,\frac{\mathrm{Im}(\overline{\mathbf{w}}\mathbf{w}')}{|\mathbf{w}|^4}\,. \tag{19.26}$$

In §19.2 a one–to–one correspondence between regular polynomial curves and regular PH curves was established by requiring the hodographs $\mathbf{w}(t)$ and $\hat{\mathbf{w}}(t)$ of corresponding curves $\mathbf{r}(t)$ and $\hat{\mathbf{r}}(t)$ to satisfy $\hat{\mathbf{w}}(t) = \mathbf{w}^2(t)$. We now compare the geometrical properties of corresponding curves.

Parametric Speed and Arc Length

The *unit–speed points* of a curve are identified by the t values (if any) where the parametric speed satisfies $\sigma(t) = 1$. In the vicinity of such points, the curve parameter t approximates the arc length s. Unit–speed points correspond to t values for which $\mathbf{r}'(t) = \mathbf{w}(t) = u(t) + \mathrm{i}\,v(t)$ crosses or touches the unit circle $u^2 + v^2 = 1$ in the hodograph plane. For polynomial curves (except straight lines) the unit–speed points must be finite in number, since it is impossible to satisfy $u^2(t) + v^2(t) \equiv 1$ unless $u(t)$, $v(t)$ are both constants — the hodograph then degenerates to just a single point, defining a straight line (the same is also true for *rational* curves: see §16.1).

Remark 19.6 The unit–speed points of a regular polynomial curve $\mathbf{r}(t)$ and its PH counterpart $\hat{\mathbf{r}}(t)$ are in one–to–one correspondence.

This follows from the fact that corresponding curves $\mathbf{r}(t)$ and $\hat{\mathbf{r}}(t)$, with hodographs $u(t) + \mathrm{i}v(t)$ and $u^2(t) - v^2(t) + \mathrm{i}\,2u(t)v(t)$, have speeds

$$\sigma(t) \,=\, \sqrt{u^2(t) + v^2(t)} \qquad \text{and} \qquad \hat{\sigma}(t) \,=\, u^2(t) + v^2(t)\,. \tag{19.27}$$

Hence the unit–speed points of $\mathbf{r}(t)$ and $\hat{\mathbf{r}}(t)$ occur at identical values of t — namely, at the (real) roots of the polynomial

$$P(t) \,=\, u^2(t) + v^2(t) - 1\,. \tag{19.28}$$

For curves of degree n and $\hat{n} = 2n - 1$, there are at most $2n - 2$ of them. A unit–speed point is "simple" if it is not a multiple root of $P(t)$.

Definition 19.1 *A segment $t \in [\,a, b\,]$ of a regular curve $\mathbf{r}(t)$ with no interior unit–speed points is* "slow" *or* "fast" *according to whether $\sigma(t) < 1$ or $\sigma(t) > 1$.*

The (odd–multiplicity) unit–speed points of a curve delimit slow and fast segments of greatest extent on it. For corresponding curves $\mathbf{r}(t)$ and $\hat{\mathbf{r}}(t)$, the slow and fast segments are in one–to–one correspondence, and if $t = a$, $t = b$ are consecutive unit–speed points on $\mathbf{r}(t)$ and $\hat{\mathbf{r}}(t)$, then for $t \in (a, b)$ we have $\hat{\sigma}(t) < \sigma(t)$ for a slow segment, and $\hat{\sigma}(t) > \sigma(t)$ for a fast segment. In other words, compared to $\mathbf{r}(t)$, the PH curve $\hat{\mathbf{r}}(t)$ is *slower* on slow segments and *faster* on fast segments: the speed variations of $\hat{\mathbf{r}}(t)$ are "exaggerated" relative to those of $\mathbf{r}(t)$. Since the arc length of any segment $t \in [\,a, b\,]$ is the integral of the parametric speed over that interval, the lengths of such segments on corresponding curves satisfy the inequalities $\hat{S}_{\text{slow}} < S_{\text{slow}}$ and $\hat{S}_{\text{fast}} > S_{\text{fast}}$.

Tangents and Curvatures

For corresponding curves with hodographs $\mathbf{w} = u + \mathrm{i}\, v$ and $\hat{\mathbf{w}} = u^2 - v^2 + \mathrm{i}\, 2uv$, we can write the tangent and curvature at points of equal parameter value as

$$\begin{aligned} \mathbf{t} \,&=\, \frac{(u,v)}{\sqrt{u^2+v^2}} \qquad \text{and} \qquad \kappa \,=\, \frac{uv'-u'v}{(u^2+v^2)^{3/2}}\,, \\ \hat{\mathbf{t}} \,&=\, \frac{(u^2-v^2,2uv)}{u^2+v^2} \qquad \text{and} \qquad \hat{\kappa} \,=\, 2\,\frac{uv'-u'v}{(u^2+v^2)^2}\,. \end{aligned} \tag{19.29}$$

Now for each t, the tangent $\hat{\mathbf{t}}$ to $\hat{\mathbf{r}}(t)$ has an inclination angle *twice* that of the tangent $\mathbf{t}$ to $\mathbf{r}(t) : \hat{\psi} = 2\,\psi$ (modulo 2π). Thus, horizontal *and* vertical tangents on $\mathbf{r}(t)$ are mapped to horizontal tangents of $\hat{\mathbf{r}}(t)$, while vertical tangents on $\hat{\mathbf{r}}(t)$ correspond to tangent angles $\psi = (2k+1)\pi/4$ for $k = 0, 1, 2, 3$ on $\mathbf{r}(t)$. Note also that the *rotation indices* of the curves

$$\mathcal{R} \,=\, \frac{1}{2\pi}\int_a^b \kappa\;\mathrm{d}s \qquad \text{and} \qquad \hat{\mathcal{R}} \,=\, \frac{1}{2\pi}\int_a^b \hat{\kappa}\;\mathrm{d}\hat{s} \tag{19.30}$$

satisfy $\hat{\mathcal{R}} = 2\mathcal{R}$ for any interval $t \in [\,a, b\,]$ — as can be verified from expressions (19.29) and the relations $\mathrm{d}s = \sqrt{u^2+v^2}\,\mathrm{d}t$ and $\mathrm{d}\hat{s} = (u^2+v^2)\,\mathrm{d}t$. These indices indicate the (net) fraction of a full circle that the curve tangent rotates through along $\mathbf{r}(t)$ and $\hat{\mathbf{r}}(t)$ — their evaluation is described in Chap. 25.

Lemma 19.2 *Inflections on* $\mathbf{r}(t)$ *and* $\hat{\mathbf{r}}(t)$ *are in one–to–one correspondence.*

Proof : Inflections are points where the curvature changes sign. From (19.29) the parameter values identifying inflections on $\mathbf{r}(t)$ and $\hat{\mathbf{r}}(t)$ must be roots of

$$u(t)v'(t) - u'(t)v(t) \,=\, 0\,. \tag{19.31}$$

To qualify as inflections, the first non–vanishing derivative of κ and $\hat{\kappa}$ at such values must be of *odd* order. Re–writing relations (19.29) as

$$\hat{\kappa} \,=\, \frac{2}{\sqrt{u^2+v^2}}\,\kappa \qquad \text{and} \qquad \kappa \,=\, \frac{\sqrt{u^2+v^2}}{2}\,\hat{\kappa} \tag{19.32}$$

and differentiating, the r–th derivative $\hat{\kappa}^{(r)}$ of the curvature of $\hat{\mathbf{r}}(t)$ is obtained as a homogeneous linear combination of the curvature κ of $\mathbf{r}(t)$ and its first r derivatives $\kappa', \ldots, \kappa^{(r)}$ — and vice–versa. For $r = 1$, we have

$$\hat{\kappa}' = 2\,\frac{(u^2+v^2)\kappa' - (uu'+vv')\kappa}{(u^2+v^2)^{3/2}}\,, \qquad \kappa' = \frac{(u^2+v^2)\hat{\kappa}' + (uu'+vv')\hat{\kappa}}{2\sqrt{u^2+v^2}}\,,$$

while higher derivatives incur more complicated expressions. Thus, at any root of equation (19.31), where $\kappa = \hat{\kappa} = 0$, we see that

$$\kappa = \kappa' = \cdots = \kappa^{(r)} = 0 \quad \iff \quad \hat{\kappa} = \hat{\kappa}' = \cdots = \hat{\kappa}^{(r)} = 0\,,$$

$\kappa^{(r+1)}$ and $\hat{\kappa}^{(r+1)}$ being non-zero. Inflections correspond to odd r values. ∎

Corresponding points of $\mathbf{r}(t)$ and $\hat{\mathbf{r}}(t)$ where $\kappa = \hat{\kappa} = 0$ but the curvatures have *even* lowest–order non–vanishing derivatives are *vertices* of these curves, i.e., points where the curvature is a local extremum value (in this case, zero). However, vertices of non–zero curvature are *not* in simple correspondence, as can be seen by writing the derivatives κ' and $\hat{\kappa}'$ in terms of u and v:

$$\begin{aligned}
\kappa' &= \frac{uv''-u''v}{(u^2+v^2)^{3/2}} - 3\,\frac{(uu'+vv')(uv'-u'v)}{(u^2+v^2)^{5/2}}\,, \\
\hat{\kappa}' &= 2\,\frac{uv''-u''v}{(u^2+v^2)^2} - 8\,\frac{(uu'+vv')(uv'-u'v)}{(u^2+v^2)^3}\,,
\end{aligned}$$

from which we see that κ' and $\hat{\kappa}'$ do not, in general, vanish simultaneously at points where $uv' - u'v \neq 0$ — i.e., where κ and $\hat{\kappa}$ are non–zero.

Remark 19.7 Inflections delineate corresponding maximal *convex segments* on $\mathbf{r}(t)$ and $\hat{\mathbf{r}}(t)$ — by "convex" we mean that the curvature is of constant sign (such segments may exhibit loops or spiral around themselves).

The correspondence of inflections on $\mathbf{r}(t)$ and $\hat{\mathbf{r}}(t)$ can also be understood geometrically. Consider a rotating line $\mathbf{l}$ through the origin of the hodograph plane. If $\mathbf{l}$ meets the hodograph $\mathbf{w}(t) = \mathbf{r}'(t)$ tangentially — and locally on one side — at $t = t_0$, the point $\mathbf{r}(t_0)$ is an inflection (see §13.5): interpreting $\mathbf{r}(t)$ vectorially, we note that $\mathbf{r}'(t_0)$ and $\mathbf{r}''(t_0)$ are parallel, and thus κ vanishes at t_0. Since angles between loci are invariant under conformal maps (see §4.5), the line $\hat{\mathbf{l}} = \mathbf{l}^2$ meets the hodograph $\hat{\mathbf{w}}(t) = \mathbf{w}^2(t)$ tangentially at $t = t_0$. Thus, $\hat{\mathbf{r}}(t_0)$ is an inflection point of the PH curve corresponding to $\mathbf{r}(t)$.

Finally, we consider the *magnitudes* of the curvatures of $\mathbf{r}(t)$ and $\hat{\mathbf{r}}(t)$ at corresponding points. We have noted that the unit circle ($\sigma^2 = \hat{\sigma} = 1$) in the $\mathbf{w}$ and $\hat{\mathbf{w}}$ hodograph planes plays an important role in determining the arc lengths of corresponding segments on $\mathbf{r}(t)$ and $\hat{\mathbf{r}}(t)$. In comparing curvatures, the circles $\sigma^2 = \hat{\sigma} = 4$ play a similar role — from (19.29) we have $|\hat{\kappa}(t)| > |\kappa(t)|$ when $\sigma^2(t) = \hat{\sigma}(t) < 4$ and $|\hat{\kappa}(t)| < |\kappa(t)|$ when $\sigma^2(t) = \hat{\sigma}(t) > 4$.

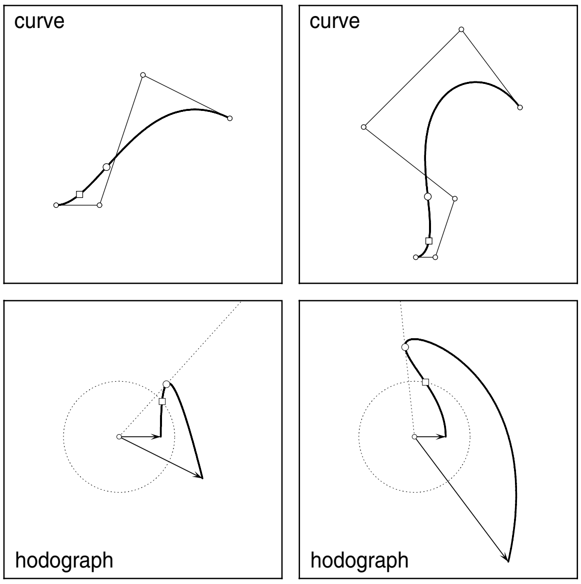

Fig. 19.5. Corresponding cubic (left) and PH quintic (right) for Example 19.2. Unit speed points (squares) arise when the hodograph crosses the circle $\sigma = 1$. Inflections (circles) arise when a radial line through the origin is tangent to the hodograph.

Example 19.2 Consider the regular cubic $\mathbf{r}(t)$ defined by control points $\mathbf{p}_0 = 0$, $\mathbf{p}_1 = \frac{1}{4}$, $\mathbf{p}_2 = \frac{1}{2} + \frac{3}{4}\,\mathrm{i}$, $\mathbf{p}_3 = 1 + \frac{1}{2}\,\mathrm{i}$. The corresponding PH quintic $\hat{\mathbf{r}}(t)$ has control points $\mathbf{p}_0 = 0$, $\mathbf{p}_1 = 9/80$, $\mathbf{p}_2 = (18 + 27\,\mathrm{i})/80$, $\mathbf{p}_3 = (-24 + 60\,\mathrm{i})/80$, $\mathbf{p}_4 = (21 + 105\,\mathrm{i})/80$, $\mathbf{p}_5 = (48 + 69\,\mathrm{i})/80$. The curves and their hodographs are illustrated in Fig. 19.5. Up to a constant factor, the polynomial (19.28) whose roots identify unit–speed points of $\mathbf{z}(t)$ and $\hat{\mathbf{z}}(t)$ is

$$P(t) \;=\; 550\,t^4 \;-\; 756\,t^3 \;+\; 342\,t^2 \;-\; 7\,,$$

and this has just one real root, $\alpha \approx 0.18$, on $t \in [\,0,1\,]$. Thus, the subsegments $t \in [\,0,\alpha\,]$ and $t \in [\,\alpha,1\,]$ are “slow” and “fast” on both $\mathbf{r}(t)$ and $\hat{\mathbf{r}}(t)$. For the PH quintic $\hat{\mathbf{r}}(t)$, the arc length of the slow/fast segment is smaller/greater than that of the cubic $\mathbf{r}(t)$. Both $\mathbf{r}(t)$ and $\hat{\mathbf{r}}(t)$ have just one real inflection for $t \in [\,0,1\,]$, at $\beta \approx 0.37$, and since the hodographs $\mathbf{w}(t)$ and $\hat{\mathbf{w}}(t)$ lie inside the circles $\sigma^2 = \hat{\sigma} = 4$, we have $|\hat{\kappa}(t)| > |\kappa(t)|$ for all $t \in [\,0,1\,]$ except $t = \beta$.